International Journal of Environmental Science and Technology
https://doi.org/10.1007/s13762-024-05958-1

ORIGINAL PAPER

Enhancing hexavalent chromium removal from textile effluent with low-cost adsorbent: simulation and a techno-economic study

F. Esmati[1] · M. C. Holliday[1,2] · S. H. Zein[1] · K. J. Jabbar[1] · S. H. Tan[3] · A. Putranto[4]

Received: 30 October 2023 / Revised: 27 March 2024 / Accepted: 11 August 2024

Abstract

This paper simulated hexavalent chromium (Cr(VI)) adsorption using cocoa pod husk biosorbent in a fixed bed column using Aspen Adsorption. This study was designed to show the effectiveness of computational methods in designing, optimising and evaluating the scaled-up adsorption process using low-cost adsorbents. To the best of our knowledge, the economic analysis of Cr(VI) removal using biosorbent adsorption columns with the assistance of Aspen Adsorption and response-surface methodology (RSM) has not been performed previously. Design Expert and RSM were used to optimise and describe the effect of flow rate and initial concentration on breakthrough and saturation times. The breakthrough time was improved by a higher bed height (2.0 m), a wider diameter (2.0 m), and lowering the flow rate (0.010 L/s). The initial concentration had no effect (1.00 mol/L). The predicted breakthrough and saturation time were 29,360 s and 313,351 s, respectively. Two scenarios were economically compared over 20 years. Scenario 1 (1-day breakthrough time) costs $746,585 and Scenario 2 (4-week breakthrough time) costs $1,538,319. This is because Scenario 2 used a taller, wider column which required a greater amount of adsorbent, and 387,873 m^3 of water were processed, respectively. Processed water was dependent on the flow rate and breakthrough time. It was concluded that cocoa pod husk could be an efficient adsorbent and the adsorption process can be successfully simulated and optimised. The use of alternative low-cost adsorbents should be encouraged. The economic study showed that simulation and RSM data could successfully be used for economic analysis.

Graphical abstract

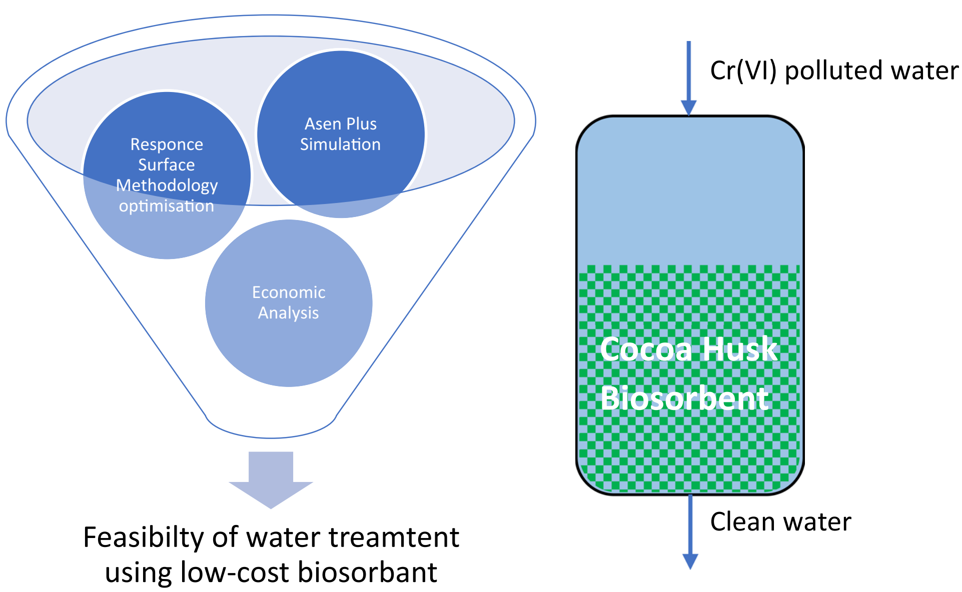

Editorial responsibility: S.Mirkia.

Extended author information available on the last page of the article

Published online: 10 September 2024

Keywords Cr(VI) · Aspen adsorption · Design expert · RSM · Biosorbent · Wastewater treatment

Introduction

Rapid industrialisation and global population growth have led to increased environmental issues like surface and groundwater pollution from untreated wastewater discharge (Carvalho et al. 2011). The continuous release of untreated wastewater exacerbates water-related problems (Bawawi et al. 2022), often due to human exposure through incomplete treatment or raw sewage reuse (Guwsmi et al. 2022). Textile industries, major water and chemical consumers, use 2–200 L of water per kilogram of fibre/fabric, with many neglecting waste management (Dawodu et al. 2020; Johanto et al. 2014; Yaseen et al. 2019). Effluents from these industries contain organic/inorganic dyes and heavy metal traces (Priyadharshini et al. 2021), posing an ecological challenge to minimise pollutants like dyes and toxic metals (Holkar et al. 2016). Industrial development has led to a rise in heavy metal pollutants in ecosystems, posing severe hazards to nature and human health (Rafiaee et al. 2020). Lead (Pb), chromium (Cr), cadmium (Cd), copper (Cu), and nickel (Ni) are commonly used in textile dyes, contributing to these issues (Priyadharshini et al. 2021; Calero et al. 2009). Heavy metals bioaccumulate and magnify in living tissues, persisting in the environment and posing challenges for biodegradation (Dawodu et al. 2020; Agarwal et al. 2022; Nwabanne et al. 2011). They enter the human body through various routes and can cause a range of toxic effects, including carcinogenic, mutagenic, and teratogenic properties (Dawodu et al. 2020; Priyadharshini et al. 2021).

Textile effluents, along with wastewater from industries like cement, mining, and electroplating, are significant sources of hexavalent chromium (Cr(VI), a highly toxic heavy metal used extensively in textile production (Dawodu et al. 2020; Guo et al. 2020; Sarkar and Das 2016). Cr(VI) compounds, including chromic acid and dichromate, pose severe health risks such as carcinogenicity, mutagenicity, respiratory issues, kidney and liver damage, lung cancer, foetal growth inhibition, skin ulceration, pulmonary congestion, and impacts on male reproductive health (Johanto et al. 2014; Calero et al. 2009; Chen et al. 2010; González-Delgadoa et al. 2022). Elevated Cr(VI) levels (>2 mg/L) hinder plant growth, seed germination, and photosynthesis while altering chloroplast structure (Johanto et al. 2014). Classified as a Group 1 carcinogen by the International Agency for Research on Cancer (IARC), Cr(VI) concentrations in industrial wastewater range from 0.5 to 270 mg/L (Dawodu et al. 2020; Priyadharshini et al. 2021; Sarkar and Das 2016). The World Health Organisation (WHO) recommends Cr(VI) levels in drinking and surface water not exceed 0.05 mg/L, while the US Environmental Protection Agency sets a limit of 0.1 mg/L for inland and potable water (Chen et al. 2010).

Various methods exist for treating wastewater, such as ultrafiltration, coagulation, flocculation, complexation, solvent extraction, flotation, reverse osmosis, ion exchange, membrane separation, electro-dialysis, precipitation, and adsorption (Carvalho et al. 2011; Dawodu et al. 2020; Priyadharshini et al. 2021). However, these approaches can be costly, energy-intensive, and less effective at low pollutant concentrations (Dawodu et al. 2020; Calero et al. 2009). A pilot-scale photo algal-bacterial treatment with dissolved air flotation has succeeded in water treatment (Bawawi et al. 2022). However, scaling up may incur high costs due to the need for consistent lighting to support algae. Photocatalysts offer promise for wastewater treatment, using reactive radicals and light absorption to break down pollutants (Saleh et al. 2023). Some, like metal oxides, work only under UV light, while others face issues like accumulation and metal ion dissolution (Saleh et al. 2023; Shahzad et al. 2022). Activated carbon support could address these issues, but it adds costs and requires intense processing (Saleh et al. 2023). Complex processes may not be viable in rural areas. Adsorption effectively removes wastewater pollutants due to its low cost, high removal capacity, ease of regeneration, and minimal secondary pollution (Carvalho et al. 2011; Priyadharshini and Soundhirajan 2021; Agarwal et al. 2022; González-Delgadoa et al. 2022; Upadhyay et al. 2023). It cleans, deodorises, detoxifies, and separates hazardous substances from aqueous solutions (Crini et al. 2018), playing a crucial role in industries like textiles and paints (Badawi et al. 2021). However, adsorption is less effective at low pollutant concentrations, and desorption of adsorbed pollutants can occur (Kenfoud et al. 2020). Proper disposal of spent adsorbents is essential for environmental safety. Combining adsorption with photocatalysis is recommended for pollutant removal and decomposition (Baaloudj et al. 2023). Selecting the right adsorbent is critical; for instance, a study successfully used low-cost biosorbent from pea waste for dye adsorption (Holliday et al. 2022a), while hydrochar from waste biomass had limited adsorption capacities (Holliday et al. 2022b).

Adsorption involves molecules binding to the surface of an adsorbent, influenced by solution pH, adsorbent dosage, particle size, initial concentration, contact time, and temperature (Anisuzzaman et al. 2016; Upadhyay et al. 2023). Activated carbon (AC) is the most versatile adsorbent for removing various pollutants from water efficiently (Dichiara et al. 2015). However, its high cost drives the search for low-cost alternatives (Carvalho et al. 2011; Nwabanne et al. 2011). AC production demands high temperatures and long activation times and necessitates thorough washing to remove chemical agents, with no possibility of regeneration (Maiti et al. 2007; Agarwal et al. 2022). Biomass polyaniline composites effectively adsorb pollutants like Cr(VI) (Rafiaee et al. 2020; Hosseini et al. 2021; Samani et al. 2019). Polyaniline's nitrogen-based unpaired electrons create negatively charged sites that attract positively charged metal ions (Rafiaee et al. 2020). However, its powdered form limits application in column systems, necessitating solid support like waste biomass (Samani et al. 2019). Biomass supports such as eggshells, feathers, fruit peel, and sawdust enhance the adsorption capacity of polyaniline, up to four times greater than raw biomass alone (Rafiaee et al. 2020; Hosseini et al. 2021; Samani et al. 2019; Ehsanpour et al. 2023). Despite their effectiveness, the complex chemical synthesis required for polyaniline composites may not be feasible in rural areas. Hence, research is underway to develop cheaper, biodegradable alternatives with high metal removal efficiency and regenerative capability (Agarwal et al. 2022). Biosorbents, derived from untreated waste biomass, offer a cost-effective and minimally processed solution for wastewater treatment. Some waste biomasses can be obtained for free, aiding in landfill reduction. Plant-based adsorbents from seeds, roots, and leaves utilise active compounds like proteins, polysaccharides, lignin, and tannins to bind and remove dyes and heavy metals from wastewater (Badawi et al. 2023). While not as efficient as AC and photocatalysts, biosorbents are simpler and less expensive to produce, making them particularly valuable in developing countries facing widespread water pollution. They exhibit good metal binding abilities (Agarwal et al. 2022). Agricultural waste material serves as an economical and environmentally friendly adsorbent, contributing to waste reduction, recovery, and reuse (Priyadharshini et al. 2021; Lingamdinne et al. 2021). After use, biosorbents can be disposed of through incineration or pyrolysis to eliminate organic compounds or utilised as soil fertiliser (Badawi et al. 2023). However, biosorbents face challenges like inconsistent properties and lack of standardisation due to variations in biomass composition and quality (Badawi et al. 2023). Studies have explored the removal of Cr(VI) from aqueous systems, achieving success with various materials. AC derived from neem leaves, garlic husk, heinsia crinita seed, coconut shells, corn stalk biochar, and modified waste wheat straw have demonstrated effective Cr(VI) removal (Dawodu et al. 2020; Guo et al. 2020; Sarkar and Das 2016). Additionally, photocatalysts have proven effective in removing Cr(VI) from wastewater (Kenfoud et al. 2020).

Computational methods offer a flexible and user-friendly approach to research, contributing to the sustainable development of the water treatment industry by saving time, effort, and experimentation costs (Mater et al. 2023). Experimental approaches may limit the evaluation of crucial operating conditions for packed bed column design (González-Delgadoa et al. 2022). Aspen Adsorption enables trials across various settings to determine optimal parameters (Anisuzzaman et al. 2016; Yasir et al. 2023; Hameed et al. 2019). Previous studies have successfully simulated the adsorption process of Cr(VI) and other pollutants (Agarwal et al. 2022; González-Delgadoa et al. 2022; Anisuzzaman et al. 2016; Nieva et al. 2019), providing a valuable alternative to time-consuming experiments for analysing potential adsorbents. Such simulation, particularly of scaled-up processes and operating condition effects, is beneficial for small and medium industries unable to afford more advanced water treatment methods (Nieva et al. 2019). Response Surface Methodology (RSM) is a statistical and mathematical approach enabling the analysis and optimisation of factor interactions under various conditions, overcoming limitations of experimental studies (Amiri et al. 2018). It aids in designing experiments to maximise resources and minimise time. RSM has effectively optimised adsorption data in various studies (Upadhyay et al. 2023; Holliday et al. 2022b; Anisuzzaman et al. 2016; Yasir et al. 2023; Sutradhar et al. 2019), with Design Expert being a successful RSM software package (Upadhyay et al. 2023; Anisuzzaman et al. 2016). Computer simulations and optimisations allow predicting industrial behaviour without building physical facilities, aiding in economic analysis for rapid cost estimates and evaluation of proposed processes (Loh et al. 2002). Factored estimation methodology is useful when specific process and technical details are lacking, assisting in performance and evaluation of chemical process equipment cost estimates (Loh et al. 2002).

To our knowledge, economic analysis of Cr(VI) removal using a biosorbent adsorption column with Aspen Adsorption and RSM assistance hasn't been conducted before.

This study demonstrates how computer software can simulate Cr(VI) adsorption and analyse the results, effectively comparing adsorption conditions and optimising the process. This enables detailed economic analysis of scenarios that would be unsafe or costly in real life. Objectives included: (1) Using Aspen Adsorption to simulate Cr(VI) removal from textile effluents using low-cost cacao pod husk, generating breakthrough curves indicating saturation and breakthrough points. (2) Optimising simulation results with Design Expert and RSM to maximise breakthrough and saturation times by studying the relationship between flow rate, bed height, bed diameter, and initial Cr(VI) concentration. (3) Utilising simulation and RSM data to develop a techno-economic approach for two differently scaled scenarios.

Materials and methods

The mechanism for Cr(VI) adsorption has been described in other sources. Oxygen containing functional groups such as hydroxyl and carboxyl and aromatic groups containing π-electrons in the adsorbent reduce the Cr(VI) to Cr(III) through electrostatic attraction and redox reactions (Guo et al. 2020). The reduced Cr(III) is dissociated into the solution via electrostatic repulsion. This mechanism is represented in the model using the Freundlich isotherm and adsorption kinetics.

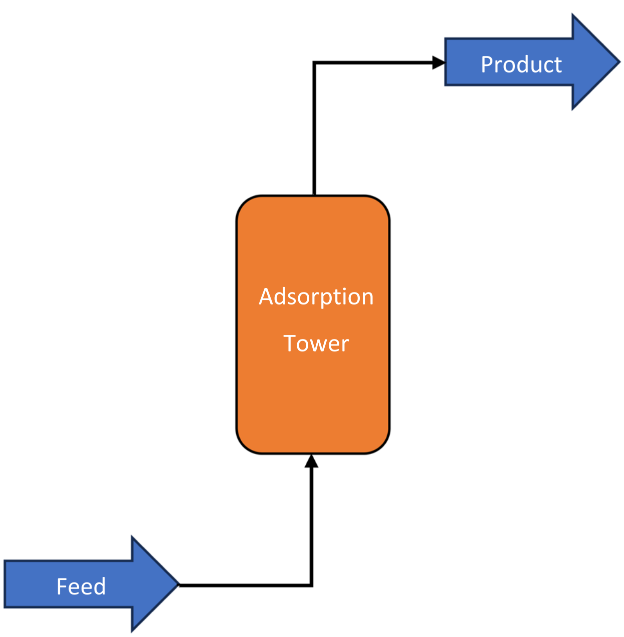

Fig. 1 Aspen adsorption flowsheet

Simulation

The simulation was performed using Aspen Adsorption. Aspen Adsorption is a flowsheet simulator for the simulation, optimisation, and analysis of gas and liquid processes. The process involves an input stream (feed), an adsorption tower, and a product stream, as shown in Fig. 1.

Component

Aspen Properties®V11 provides access to the chemical and physical properties of Cr(VI), such as the electrolyte reaction, equilibrium constants and stoichiometry (Nieva et al. 2019). Aspen Adsorption gives the physical properties of any electrolyte when combined with water. There is no need to add H_2O to the components (Nieva et al. 2019). The component representing Cr(VI), was named "CRO4-2". The method chosen is ELECNRTL, (Electrolyte Non-Random Two Liquid) because it is flexible and can be used for high or low concentrations. It is also the best way to estimate liquid electrolyte solutions if no vapour phase is involved (Agarwal et al. 2022; Nieva et al. 2019).

Fixed bed

The selected adsorbent was cocoa husk from Theobroma Cacao. A detailed characterisation of waste biomass has been performed in our previous studies, employing techniques such as Fourier-transform infrared spectroscopy, thermogravimetric analysis and scanning electron microscope with energy dispersive X-ray (Holliday et al. 2022a, b). There was one adsorbent layer within the bed. The bed porosity, constant mass transfer coefficient and Freundlich isotherm data for the cocoa husk adsorbents were acquired from a different study (González-Delgadoa et al. 2022). The properties of cocoa pod husk can be seen in Table 1.

The value 1/n is the adsorption intensity, indicating the favourability of adsorption (Chen et al. 2010). A value of 1/n less than 1 indicates normal adsorption but a value over 1 indicates the process is cooperative adsorption (Dawodu et al. 2020). Cooperative adsorption is when the adsorption of one molecule enhances the adsorption of

Table 1 Cocoa pod husk adsorbent parameters (González-Delgadoa et al. 2022)

Property	Value
Bulk density (kg/m^3)	518
Particle size (μm)	500
Constant mass transfer coefficient (1/s)	3.2×10^{-10}
Freundlich isotherm constant [(mg g^{-1}) (mg L^{-1}) $^{-1/n}$]	8.69
1/n	1.53

additional molecules. Because the isotherm data has only been provided for a single temperature, any changes in the model temperature will have no effect on the breakthrough times. Isothermal data for each temperature range would be required to document changes caused by temperature. However, it is recognised temperature will have a significant effect on the adsorption process and would be considered in future work. The bed has a variable height and diameter, an interparticle voidage of 0.25 (m^3 void/m^3 bed), a solid density of 518 kg/m^3 and a constant mass transfer coefficient of $3.2e^{-10}$ 1/s. A variable bed height of 0.5, 1.0 and 2.0 m and bed diameter of 0.5, 1.0 and 2.0 were selected based on the values used in other similar studies (Agarwal et al. 2022; Upadhyay et al. 2023; Anisuzzaman et al. 2016). Many independent studies were analysed in order to obtain the best assumptions for the simulation. Below are all the assumptions:

- The bed orientation was vertical upward flow (Agarwal et al. 2022).
- The fluid behaves as a plug flow with axial dispersion. Since ideal mixing is assumed, molar concentrations can be calculated using molar volume. Isothermal conditions apply (Upadhyay et al. 2023).
- Used the upwind differencing scheme 1 (UDS1). UDS1 is based on the first-order Taylor expansion (Agarwal et al. 2022; Upadhyay et al. 2023; Anisuzzaman et al. 2016; Nieva et al. 2019).
- Used 20 nodes, the same value as in other studies (Upadhyay et al. 2023; Nieva et al. 2019).
- The material balance is convection and constant dispersion (González-Delgadoa et al. 2022).
- No pressure drop (González-Delgadoa et al. 2022; Anisuzzaman et al. 2016).
- Constant velocity (González-Delgadoa et al. 2022).
- Adsorption of the liquid phase is negligible since only a small amount of concentration is used (Zhang et al. 2019).
- The film model was assumed to be solid. The mass transfer force is expressed in terms of solid phase concentrations (Agarwal et al. 2022; Upadhyay et al. 2023; Nieva et al. 2019; Zhang et al. 2019).
- A linear lumped resistance kinetic model (Agarwal et al. 2022; González-Delgadoa et al. 2022; Upadhyay et al. 2023; Anisuzzaman et al. 2016; Nieva et al. 2019).
- Constant mass transfer coefficient (González-Delgadoa et al. 2022; Zhang et al. 2019).
- Freundlich 1 isotherm (González-Delgadoa et al. 2022; Lingamdinne et al. 2021; Nieva et al. 2019).
- The energy balance was isothermal (González-Delgadoa et al. 2022; Anisuzzaman et al. 2016; Zhang et al. 2019).

A partial differential mass balance can be used to express the metal ion concentration in a small volume inside the adsorbent bed, this can be seen in Eq. 1 (Upadhyay et al. 2023).

$$-\varepsilon_i E_z \frac{\partial^2 C}{\partial Z^2} + \frac{\partial\left(v_i C\right)}{\partial Z} + \varepsilon_i \frac{\partial C}{\partial t} + \rho_s \frac{\partial q}{\partial t} = 0 \quad (1)$$

The bed porosity is ε_i, the axial dispersion is E_z (m^2/s), the liquid phase concentration is C (kg/m^3) and z is the distance along the bed in meters, v_i is the interstitial velocity of the fluid through the adsorbent bed (m/s), q is the concentration of adsorbed ions onto the adsorbent (mg/g) with $\partial q/\partial t$ being the rate of adsorption, ρ_s is the bulk density (kg/m^3) and t is time (s). The first term represents dispersive forces. The second term is convection force. The third term is used to account for ion accumulation on the adsorbent. The fourth term, mass transfer, accounts for ion transfer from the liquid to the solid phase (Agarwal et al. 2022; Upadhyay et al. 2023).

Feed and product

The feed flow rate is a variable, the concentration of Cr(VI) is variable, the temperature is 25 °C and the pressure is 1 bar. A variable flow rate of 0.010, 0.025 and 0.050 L/s was used based on the values used in other upscaled column studies (Agarwal et al. 2022; Upadhyay et al. 2023; Nieva et al. 2019). A variable initial concentration of 1.00, 0.10 and 0.01 mol/L was used based on the values used in other Cr(VI) studies, but a higher range was selected to represent an upscaled flow (Dawodu et al. 2020; Chen et al. 2010). The product stream Cr(VI) concentration is set to an initial 0 mol/L to determine the dynamic breakthrough time for the adsorption columns (Nieva et al. 2019). The model type for the process was the reversible model (Nieva et al. 2019).

Response surface methodology (RSM)

Design Expert V13 was used to investigate the interaction between the variables and optimise breakthrough and saturation times using RSM. The simulation data was fitted to a two-factor interaction mathematical model to find the equation that best describes the relationship between the variables. This equation could then be used in optimisation. The model was filtered to exclude terms with a p value greater than 0.10. A p value less than 0.05 indicates that the term is statistically meaningful, and values higher than 0.10 indicate it is not (Stat-Ease, Inc., 2021). These equations were then used to plot three-dimensional graphs that showed the relationship between variables and their effect on breakthrough and saturation time. The information obtained was used to optimise the variables to maximise breakthrough and saturation time.

Results and discussion

This section compares how the changes in flow rate, initial concentration of Cr(VI), bed height and diameter affect breakthrough and saturation time. The breakthrough occurs at a concentration of 5% effluent (C_e= 0.05 C_0) (Agarwal et al. 2022). The outflow concentration increases rapidly after this point until the bed is saturated. The saturation time is when the outflow Cr(VI) concentration reaches 95% of the input Cr(VI) concentration (C_e= 0.95 C_0), meaning the bed is saturated (Agarwal et al. 2022). The breakthrough curve plots relative concentration against time. The curve can be used to compare different adsorption profiles. It is an indicator of the performance of an adsorbed bed column. However, breakthrough time can also be affected by temperature, pH, materials properties and other factors (Agarwal et al. 2022). A longer breakthrough time is an indicator of better adsorption within the adsorption column (Nieva et al. 2019). Table 2 shows the simulation runs to examine the effects of flow rate, initial concentration of Cr(VI), bed height and diameter on breakthrough and saturation times.

Runs 1–3 investigate the effects of flow rate; runs 2, 4 and 5 investigate the effects of bed height; runs 2, 6 and 7 investigate the effects of initial concentration and runs 2, 8 and 9 investigate the effects of bed diameter. Runs 10–13 cover other data points to be used in Design Expert to investigate how the different variables interact. Decreasing the flow rate and increasing bed height and diameter will increase both breakthrough and saturation times. It can also be seen that initial concentration has a negligible effect on both times. These will be discussed in the subsequent sections. The adsorption capacity before breakthrough time was calculated from the area of the curve. Adsorption capacity is increased at higher flow rates, bed heights and concentrations where breakthrough time and the amount of material passing through the column is maximised. A lower bed diameter lowers the amount of adsorbent in the column increasing relative adsorption efficiency.

The effect of flow rate on breakthrough and saturation times

Better performance was observed at lower flow rates. The column bed has a shorter breakthrough and saturation time at higher flow rates and a steeper curve. Figure 2 shows the breakthrough curve for different flow rates.

As shown in Fig. 2, when the flow rate decreases, the breakthrough and saturation time increases. The plot for 0.05 L/s has the highest flow rate and, therefore, the shortest breakthrough and saturation time of 553 and 1379 s, respectively. The plot for 0.01 L/s has the lowest flow rate and, therefore, the longest breakthrough and saturation time of 2177 and 7539 s, respectively. Similar results were seen in other studies (Calero et al. 2009; Agarwal et al. 2022; Sarkar and Das 2016; González-Delgadoa et al. 2022; Anisuzzaman

Table 2 Simulation runs and effects of flow rate, bed height, bed diameter and initial Cr(VI) concentration on the breakthrough and saturation time

Run	Flow rate (L/s)	Bed height (m)	Initial conc (mol/L)	Bed diameter (m)	Break-through (Seconds)	Saturation (Seconds)	Adsorption capacity (mg/g)
1	0.050	1.0	1.00	0.5	553	1,379	18.85
2	0.025	1.0	1.00	0.5	1,036	2,828	17.65
3	0.010	1.0	1.00	0.5	2,177	7,539	14.84
4	0.025	2.0	1.00	0.5	2,226	5,460	18.97
5	0.025	0.5	1.00	0.5	455	1,491	15.51
6	0.025	1.0	0.10	0.5	1,036	2,821	1.77
7	0.025	1.0	0.01	0.5	1,036	2,828	0.18
8	0.025	1.0	1.00	1.0	3,060	12,600	13.04
9	0.025	1.0	1.00	2.0	6,000	48,420	6.39
10	0.010	2.0	1.00	2.0	25,740	311,880	5.48
11	0.050	2.0	1.00	1.0	4,160	11,310	17.72
12	0.010	0.5	1.00	1.0	1,600	13,665	5.45
13	0.050	0.5	1.00	2.0	1,495	11,675	6.37

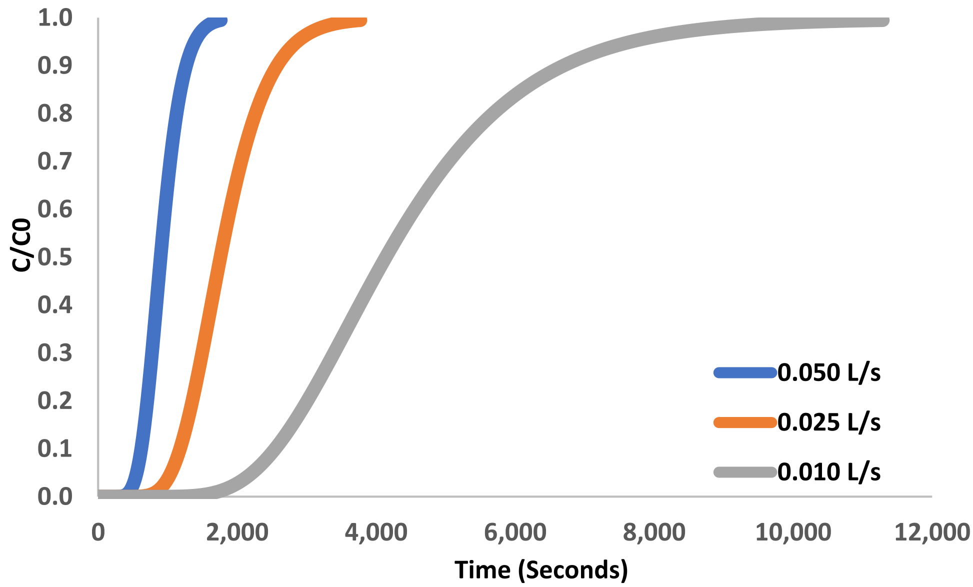

Fig. 2 Breakthrough curves of different flow rates

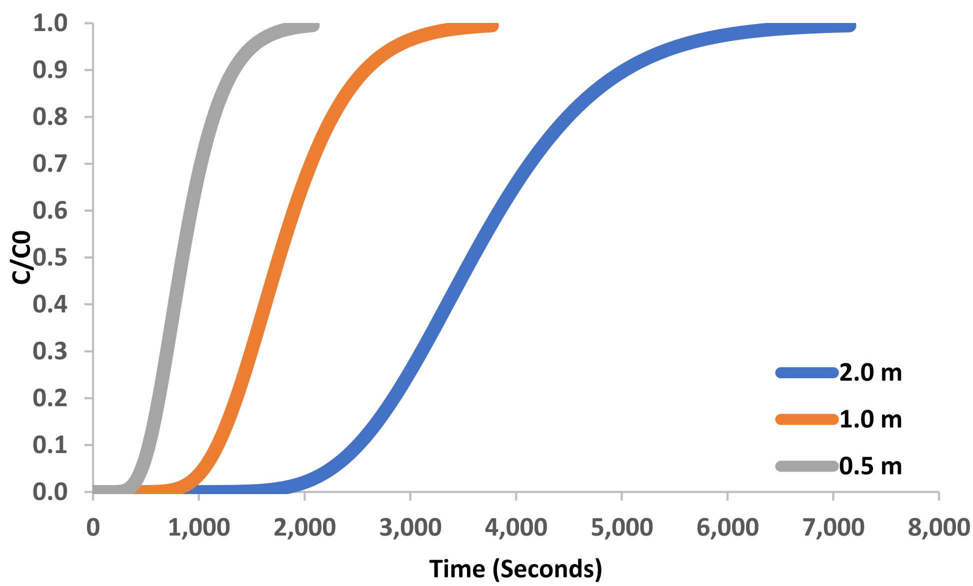

Fig. 3 Breakthrough curves of different bed heights

et al. 2016). A lower flow rate improved breakthrough and saturation time because the wastewater containing Cr(VI) had an increased contact time with the adsorbent, improving adsorption. The flow rate determines the interstitial velocity, which in turn defines the contact time between the Cr(VI), ions and the adsorbent (Agarwal et al. 2022). A lower residence time reduces the opportunity for the ions to reach the micro and mesopores in the adsorbent (Agarwal et al. 2022). Increased slopes at high flow rates may be caused by a reduction in the external film diffusion mass-transfer resistance (Agarwal et al. 2022). The increased fluid movement can cause pores to clog at higher flow rates (Nieva et al. 2019). A faster flow rate means the bed will reach its capacity quicker but will increase water processing time. The main industrial considerations are balancing the volume of water that needs processing, the swiftness this needs to be processed and the cost of replacing the bed once saturated. With a cheap bed material, the cost of replacing the bed is not a significant factor.

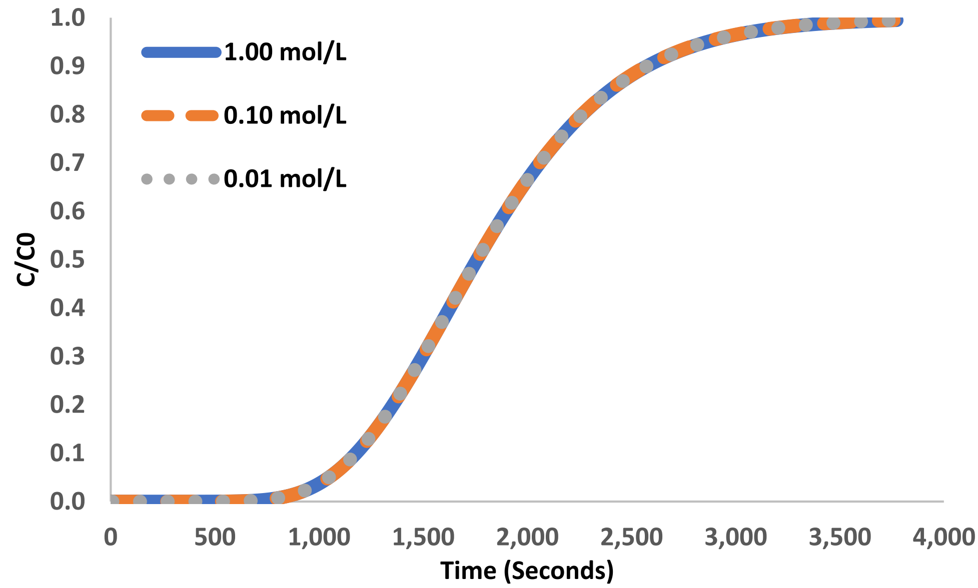

Fig. 4 Breakthrough curves of different initial concentrations of Cr(VI)

The effect of bed height on breakthrough and saturation times

Breakthrough and saturation time increase as the bed height increases. Figure 3 shows the breakthrough curve for different bed heights.

As shown in Fig. 3, when the adsorption column bed height increases, the breakthrough and saturation time also increase. This means that the plot for the tallest bed height of 2 m had the longest breakthrough and saturation time of 2226 and 5460 s, respectively. The plot for the shortest bed height of 0.5 m has the shortest breakthrough and saturation time of 455 and 1491 s, respectively. Other studies have also shown similar results (Calero et al. 2009; Agarwal et al. 2022; Sarkar and Das 2016; Anisuzzaman et al. 2016). A taller bed means more adsorption material. Higher bed heights result in a higher adsorbent dosage, which improves absorption efficiency due to additional available active sites (Lingamdinne et al., 2021; Amiri et al. 2018). At a higher bed height, diffusion mass transfer is more effective than axial dispersion, which dramatically increases breakthrough times (Agarwal et al. 2022). At a lower height, axial dispersion is the dominant mass transfer method and causes a reduction in ion diffusion (Nieva et al. 2019). A consideration for a taller bed is more absorbent material is required and a taller column will have a higher capital cost. A shorter column would cost less to manufacture and require less absorbent material, but the bed would need to be replaced more often. A low-cost bed material would remove this concern.

The effect of initial concentration of cr(VI) on breakthrough and saturation time

The initial concentration of Cr(VI) did not affect the breakthrough and saturation time in the simulation. Figure 4 shows the breakthrough curve for different initial concentrations of Cr(VI).

The initial concentration (Fig. 4) does not affect the breakthrough and saturation time. The times for breakthrough and saturation were the same, at 1,036s and 2,828s, respectively. Another study also reported similar results (Anisuzzaman et al. 2016). The authors conclude that the linear lumped resistance assumption in the kinetics models may not accurately describe the adsorption mechanism (Anisuzzaman et al. 2016). However, in other studies, linear lumped resistance was used to investigate the effects of initial saturations on breakthrough and breakthrough times (Agarwal et al. 2022; Upadhyay et al. 2023; Nieva et al. 2019). In a second study, the conclusion was that because the lumped resistance kinetic model was used and the assumption that the rate of ion uptake is directly proportional to their gradient concentration, a higher concentration will increase the exhaustion capacity (Upadhyay et al. 2023). In other studies, lower initial concentrations increased the adsorption and prolonged the saturation and breakout time (Calero et al. 2009; Agarwal et al. 2022; Sarkar and Das 2016; Lingamdinne et al. 2021; Nieva et al. 2019; Amiri et al. 2018; Zhang et al. 2019). They conclude that at higher concentrations, the number of empty adsorption sites decreases or becomes saturated with pollutant molecules. The remaining sites are less available and reduce adsorption efficiency (Amiri et al. 2018). The number of active sites was not enough to adsorb pollutants.

These other studies were examined to understand why the results of this study are different. The range of flow rates and

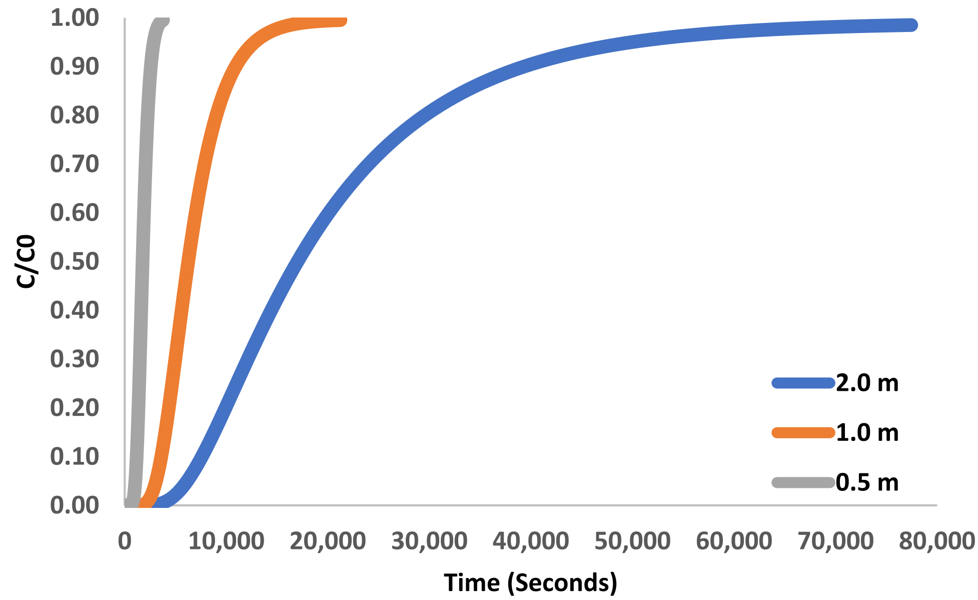

Fig. 5 Breakthrough curves of different bed diameters

initial Cr(VI) concentrations selected in the current study could explain why changing the initial Cr(VI) concentration did not change breakthrough or saturation times. The current study used a higher flow of 0.05 – 0.01 L/s with a higher initial Cr(VI) concentration of 52,000 to 520 mg/L. Other laboratory-scale studies used a significantly lower flow rate, between 0.00010 and 0.00002 L/s. This could increase the impact of the initial metal ion content on breakthrough and saturation time (Calero et al. 2009; Zhang et al. 2019). In other laboratory-scale studies, the initial concentration was 200-2 mg/L. This again increased its effect on breakthrough and saturation time (Calero et al. 2009; Agarwal et al. 2022; Nieva et al. 2019). If a considerably lower flow rate and concentration were chosen, then it is likely that the initial concentration would have a more significant effect. However, a lower flow rate and initial concentration would seriously lower the throughput of the adsorption column, greatly decreasing its functionality. Besides, the nature of the adsorbent might also affect the breakthrough and saturation times because different materials have different characteristics toward the adsorbate.

The effect of bed diameter on breakthrough and saturation time

The breakthrough and saturation times increased at wider bed diameters. Figure 5 shows the breakthrough curve for different bed diameters.

Figure 5 shows breakthrough and saturation time increase when the bed diameter increases. This means the highest breakthrough and saturation times of 6000 s and 48,420 s, respectively, are at a diameter of 2.0 m. The lowest breakthrough and saturation times of 1036 s and 2828 s, respectively, are at a diameter of 0.5 m. Similar results were found in another study (González-Delgadoa et al. 2022). The effect of bed diameter should share similar characteristics to the effect of bed height. A larger diameter inherently means a larger amount of adsorbent in the column. A larger amount of adsorbents means more adsorption sites, increasing the amount of Cr(VI) removed from the water and extending the amount of clean water passing through the column. This causes an increase in breakthrough and saturation times. The RSM will indicate if the effect of bed diameter is more or less significant than bed height. Like bed height, the main considerations are a wider column requires more absorbent material and has a greater capital cost. A narrower column will be cheaper to manufacture and require less adsorbent material, but the bed will need to be replaced more often. A low-cost adsorbent material would supersede such concerns.

After the adsorbent bed reaches full saturation, it requires disposal. An effective alternative to disposal would be the desorption of pollutant particles and regeneration of the adsorbent. The adsorbed metal can be desorbed and recovered using solutions such as hydrochloric acid (Priyadharshini and Soundhirajan 2021) or nitric acid (Dawodu et al. 2020). Notably, biosorbents have demonstrated to show high desorption efficiency (> 90%) even after three desorption cycles (Dawodu et al. 2020) indicating their potential for reuse and sustainability in pollution management practices.

Investigation of variable interaction and their optimisation using response surface methodology

The Design Expert software optimised the breakthrough time and identified the relationships between the variables flow rate, bed height, initial concentration, and bed diameter,

Table 3 Analysis of variance for the reduced two-factor interaction model

	Breakthrough time			Saturation time		
	F-value	*p* value	Significance	F-value	*p* value	Significance
Model	55.98	< 0.0001	Significant	90.30	< 0.0001	Significant
A—Flow rate	22.27	0.0011		43.71	< 0.0001	
B—Bed height	60.39	< 0.0001		34.62	0.0002	
D—Bed diameter	79.73	< 0.0001		190.04	< 0.0001	

which were given terms A, B, C and D, respectively. Design Expert recommended that a base 10-logarithmic transformation be used to better fit the dataset. Logarithmic transforms work better with data that is bounded in variance or has a high growth rate. To describe the effects of variables on breakthrough and saturation times, a reduced two-factor model was used. The model was filtered to exclude terms with a *p*-value greater than 0.10. A *p* value less than 0.05 indicates that the term is statistically meaningful and values higher than 0.10 indicate that the term is non-significant (Stat-Ease, Inc., 2021). Possible terms included A, B, CD, AB, AC, AD, BC, BD, and CD. Equations 2 and 3 show a mathematical model for the breakthrough and saturation times of each adsorbent.

$$\mathrm{Log}_{10}(\text{Breakthrough time}) = 2.57 - 11.49 \times \text{ A } + 0.50 \times \text{ B} + 0.50 \times \text{ D} \tag{2}$$

$$\mathrm{Log}_{10}(\text{Saturation time}) = 3.11 - 17.84 \times \text{ A} + 0.42 \times \text{ B} + 0.85 \times \text{ D} \tag{3}$$

These equations can be used to predict the saturation and breakthrough time. The terms C, AB, AC, AD, B, C BD, and CD are not included in either equation because their *p*-values were higher than 0.10. Initial concentration may have little impact on breakthrough and saturation times. There are no two-factor terms, which indicates that there is no interaction between factors. The analysis of variance and fit statistics have been shown to show the suitability of both models. In Table 3, you can see the analysis of variances for both reduced two-factor interaction models for saturation and breakthrough time.

The F-values for breakthrough and saturation time indicate that models are significant. A *p* value less than 0.05 indicates a significant term. The significance of all selected terms is therefore confirmed. Table 4 shows the fit statistics of two reduced two-factor interaction models for saturation and breakthrough time.

Table 4 Fit statistics

	Breakthrough time	Saturation time
R^2	0.9491	0.9678
Adjusted R^2	0.9322	0.9571
Predicted R^2	0.8852	0.9259
Adequate precision	25.4224	32.4272

The R^2, predicted R^2 values and the adjusted R^2 of both models are very close to 1, indicating the models are good predictors for the simulation results (Upadhyay et al. 2023). The predicted R^2 of both models and the adjusted R^2 are within reasonable limits, with a difference of less than 0.0200. This suggests that the current model can accurately predict responses (Stat-Ease, Inc., 2021). A ratio of greater than four is desired for 'adequate accuracy' (Stat-Ease, Inc., 2021). The ratios given indicate a good signal. In Fig. 6, you can see the 3-D graphs of the reduced two-factor interaction models for breakthrough time.

Figure 6A illustrates the impact of bed height and flow rate on breakthrough time. The highest breakthrough time is at a low flow rate and high bed height. The gradient shows that the bed height has a more significant impact on breakthrough time. Figure 6B illustrates the impact of the flow rate and diameter of the bed on breakthrough time. This graph shows a similar pattern to that of Fig. 6A. Figure 6C illustrates the effect of bed size and height on breakthrough time. It shows breakthrough time to be greatest at high bed height and diameter. The gradient shows the factors to have equal significance. Initial chromium concentration does not appear in the two-factor interaction equation and, therefore, does not feature in the 3-D plots. In another study, it was found that initial concentration and dose were significant influences on adsorption efficacy (Lingamdinne et al. 2021). In Fig. 7, you can see the 3-D graphs of the reduced two-factor interaction models for saturation time.

Figure 7A shows the effect of flow rate and bed heights on saturation times. This graph displays a pattern like that of Fig. 6A. The gradient indicates that flow rate is more important in determining saturation time. Figure 7B shows the effect of flow rate and bed diameter on saturation time. This graph displays a pattern like that of Fig. 6B. Gradients show that bed diameter has more of an effect on saturation times. Figure 7C shows the effects of bed diameter and height on saturation times. This shows a similar pattern to Fig. 6C. The bed diameter has a greater impact on saturation than breakthrough time. The initial chromium content does not figure

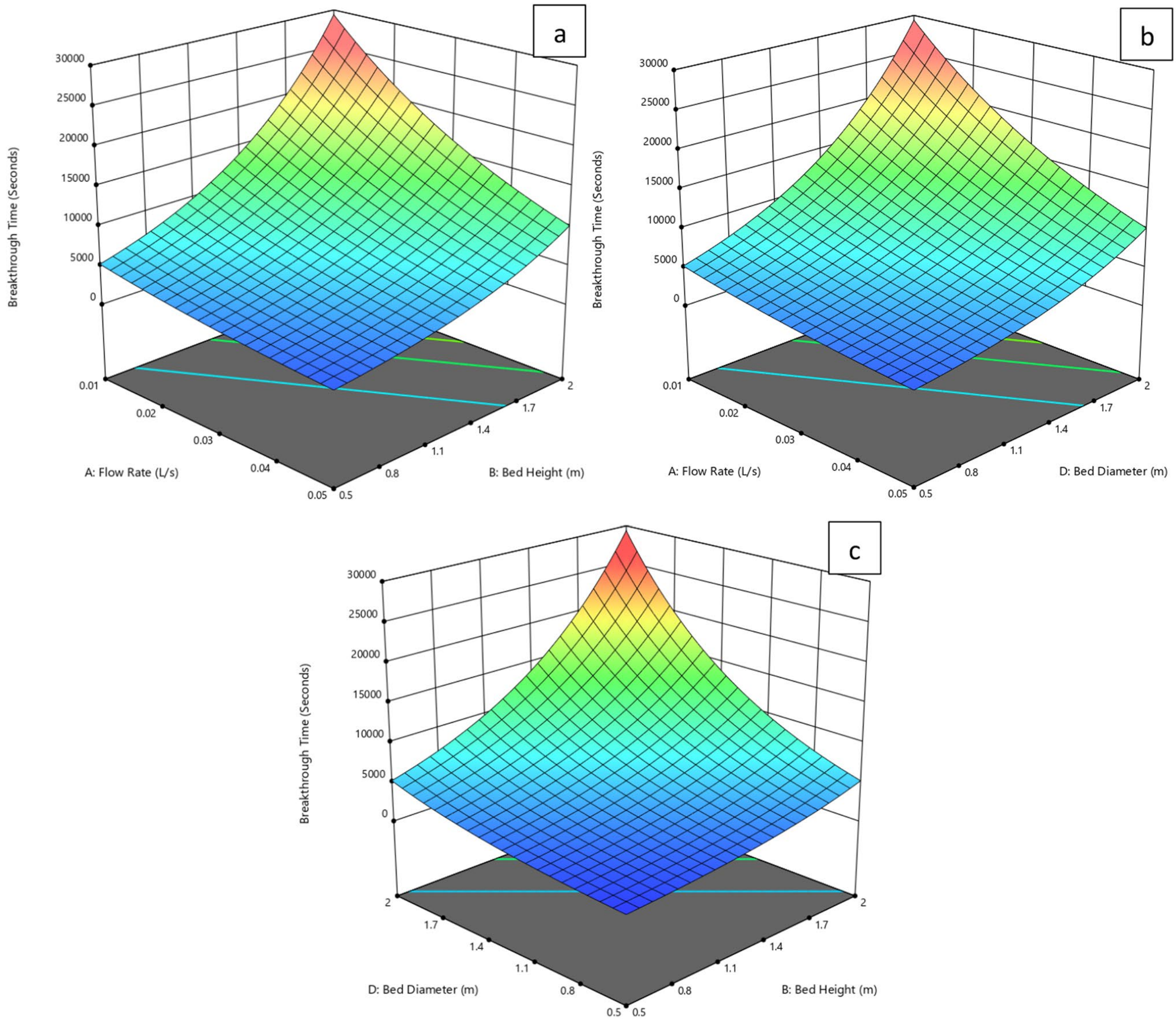

Fig. 6 Model graphs for **a** the effect of flow rate and bed height on breakthrough time, **b** the effect of flow rate and bed diameter on breakthrough time and **c** the effect of bed height and bed diameter on breakthrough time

in the equation of two-factor interactions and is, therefore, not included in the plots.

Design Expert can be used to find the optimum solution at the defined range of values to maximise breakthrough and saturation time. The optimum parameters are, therefore, a flow rate of 0.01 L/s, a bed height of 2.0 m, a bed diameter of 2.0 m and an initial concentration of 1.00 mol/L to give a predicted breakthrough and saturation time of 29,360 and 313,351 s, respectively. By using the area of the curve, the approximate adsorption capacity before the breakthrough time is 6.25 mg/g. By altering the bed height, bed diameter and flow rate the breakthrough time can be adjusted to whatever specification is required. Theoretically, with a large enough bed height and diameter and low enough flow rate the adsorbent could last for years. However, unmodified biomass is not expected to last long before deteriorating in constant wet conditions. The decomposition of cocoa pod husk has been noted not to be strongly affected by rainfall frequency and amounts (Hougni et al. 2021). In other studies on biodegradation, the mass loss of cocoa pod husk was recorded as 0.1% after 60 days and 33% after 1 year (Hougni et al. 2021; Rahim et al. 2019). It can be assumed that the biomass would last one year before requiring changing.

The practical implications of the RSM analysis reveal the significant factors and how they interact with each other. It provides insight into how the breakthrough time will react when certain factors are altered when the process is scaled up. Flow rate, bed height and diameter are

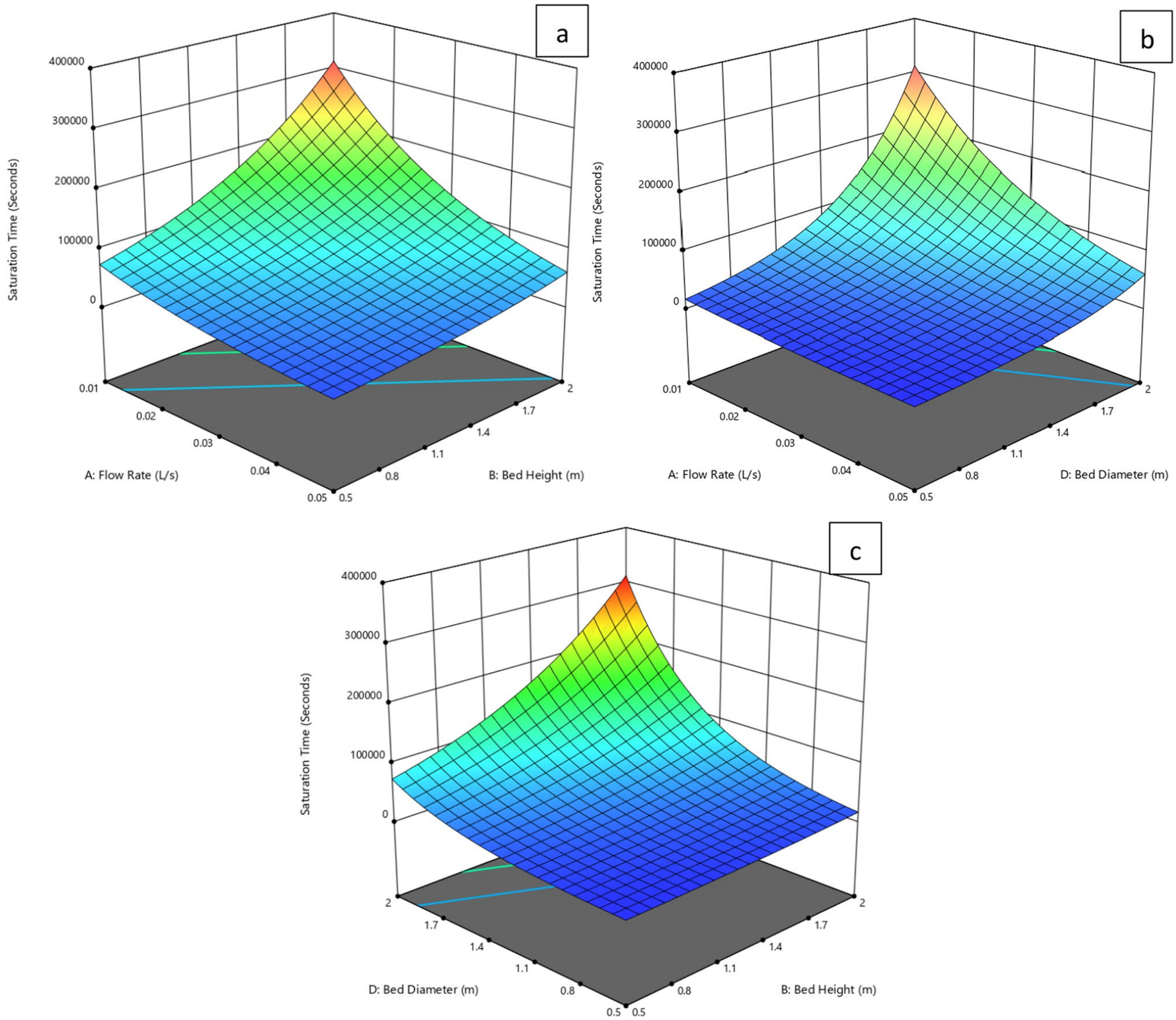

Fig. 7 Model graphs for **a** the effect of flow rate and bed height on saturation time, **b** the effect of flow rate and bed diameter on saturation time and **c** the effect of bed height and bed diameter on saturation time

all significant factors and do not interact with each other. This means, that when one factor can is scaled up it will not affect the response of the other factors. It also means changing either factor will have a significant effect on the breakthrough and saturation times. This method can be used with other adsorbents to study how they respond to changing the adsorption conditions. The software does not consider all scenarios and factors such as human error, environmental conditions or political legislation. The quality of simulations is only as good as the input data and the skills of the user.

Table 5 Scenarios for economic analysis

Scenario	Bed diameter (m(ft))	Flow rate (L/s)	Bed height (m (ft))	Initial con (mol/L)	Breakthrough (Seconds(days))	Processed water per bed (L)
1	0.305 (1)	0.045	5.486 (18)	1	86,400 (1)	3927
3	1.067 (3.5)	0.614	20.726 (68)	1	2,419,200 (28)	1,486,103

The simulation response can be relatively accurate to reality depending on the model complexity and reliability of the input data. Future work could include investigating other factors, such as the effect of temperature, the simulation of the adsorption column in series and the investigation of the adsorption of mixed pollutants. Different RSM models are available to investigate how the method affects the response.

Design Expert can be used to predict outcomes beyond the programmed range. Using Eq. 2, two scenarios were suggested. A breakthrough time of 1 day and 4 weeks. Since the initial concentration had no effect at the selected range, it was set to 1.00 mol/L for all scenarios. The 1-day scenario had a flow rate of 0.045 L/s, a bed height of 5.486 m and a bed diameter of 0.305 m to give a breakthrough time of 86,400 s. The 4-week scenario had a flow rate of 0.614 L/s, a bed height of 20.726 m and a bed diameter of 1.067 m to give a breakthrough time of 2,419,200 s. The bed height and diameter were selected based on the available cost curve for packed columns, which used units of feet. The value for flow rate was chosen to reach the necessary breakthrough time for each scenario. These two scenarios were used in economic analysis.

Economic evaluation

The economic analysis identifies favourable process scenarios (Waudby et al. 2021; Thoppil et al. 2021). In this section, the two scenarios will be investigated economically. Scenario 1 has a breakthrough time of 1 day, a bed height of 18 feet and a bed diameter of 1 feet. Scenario 2 has a breakthrough time of 4 weeks, with a bed height of 68 feet and a diameter of 3.5 feet. The scenarios will be judged over a 20-year period, which is standard for process plant economic analysis. The economic evaluation section usually comprises two categories: Capital expenditure and operational expenditure. The two scenarios are shown in Table 5.

Table 6 Cost of cocoa pod waste adsorbent per kg (Sharma et al. 2021)

Item	Unit cost ($)	Amount	Price of pod waste ($)
Drying cost	0.15/kWh	0.6 KWh, 90 °C, 5 h	0.09
Grinder	0.15/kWh	0.8 KWh, 1 h	0.12
Net cost ($)	–	–	0.21
Other overhead costs (15% of the net cost) ($)	–	–	0.03
Total cost ($/kg)	–	–	0.24

Any values in UK£ were converted to US$ at a rate of 1.2, according to the Bank of England in 2023 (Bank of England 2023).

Cost of adsorbent preparation from Cacao Pod Husk

The price of the adsorbent used to remove metals from wastewater is a major factor in the cost of the adsorption process. AC is the most widely used and expensive adsorbent for removing Cr(VI). The cost and demand for AC can be difficult for developing nations to pay. Therefore, it is imperative to find low-cost materials comparable to AC in adsorption capacity, economic viability, and local availability (Sharma et al. 2021).

Agri-waste is difficult to dispose of without causing significant harm to the environment. It is expensive to transport and is often burnt instead, releasing greenhouse gases. By using this waste to remove chromium or other heavy metals from aqueous solutions, it aids in the management of agri-waste. In addition to indirectly helping the environment and society by removing heavy metals, the application of agri-waste is beneficial to farmers since it can be repurposed and revalued. Industry benefits because heavy metals can be removed from wastewater for a cheaper cost. The low

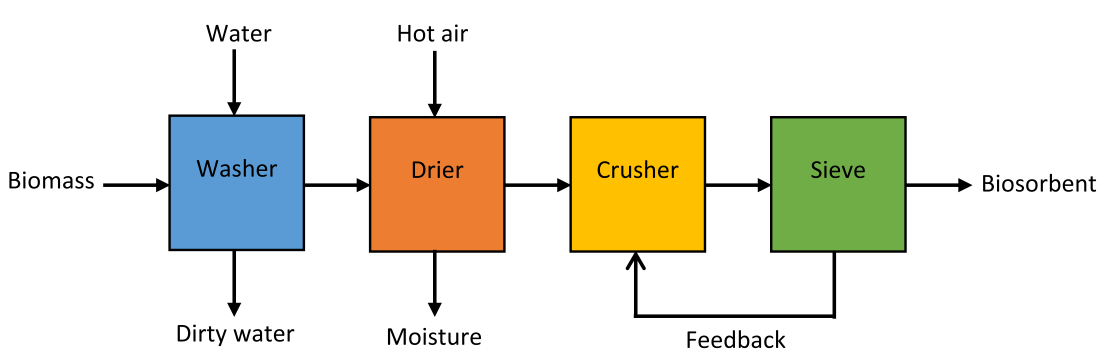

Fig. 8 Flowsheet for biosorbent production

Table 7 Equations for solving capital expenditure

Variable	Equation	Value	Eq. No.
ISBL	$ISBL = total\ installed\ equipment\ cost$	Scenario 1: \$73,000 Scenario 2: \$178,500	
Inflation factor	$ISBL_{2022} = ISBL_{1998} \times \left(\frac{index_{2022}}{index_{1998}}\right)$	Scenario 1: $73,000 \times \frac{821.3}{389.5} = \$153,928$ Scenario 2: $178,500 \times \frac{821.3}{389.5} = \$376,385$	4
OSBL	$OSBL = ISBL \times 0.4$	Scenario 1: $153,928 \times 0.4 = \$61,571$ Scenario 2: $376,385 \times 0.4 = \$150,554$	5
Contingency cost	$Contingency\ cost = (ISBL + OSBL) \times 0.1$	Scenario 1: $(153,928 + 61,571) \times 0.1 = \$21,550$ Scenario 2: $(376,385 + 150,554) \times 0.1 = \$52,694$	6
D&E cost	$\text{D\&E}\ cost = (ISBL + OSBL) \times 0.2$	Scenario 1: $153,928 + 61,571) \times 0.2 = \$43,100$ Scenario 2: $376,385 + 150,554) \times 0.2 = \$105,388$	7
FCI	$FCI = ISBL + OSBL + Contingency\ cost + \text{D\&E}\ cost$	Scenario 1: $153,928 + 61,571 + 21,550 + 43,100 = \$280,149$ Scenario 2: $376,385 + 150,554 + 52,694 + 105,388 = \$685,021$	8
WCI	$\text{WCI} = (ISBL + OSBL) \times 0.05$	Scenario 1: $153,928 + 61,571) \times 0.05 = \$10,775$ Scenario 2: $(376,385 + 150,554) \times 0.05 = \$26,347$	9
CAPEX	$\text{CAPEX} = FCI + WCI$	Scenario 1: $280,149 + 10,775 = \$290,924$ Scenario 2: $685,021 + 26,347 = \$711,368$	10

cost of the raw material reduces the overall expenses of the procedure and the final product (Sharma et al. 2021).

Adsorbent manufacturing feasibility is determined by the cost per mass of the raw materials used in the synthesis process. No thermal or chemical treatment, except drying and grinding, is required to prepare waste biomass as a biosorbent. Cacao pod husk is an abundant natural waste that can be used as an alternative to commercially used adsorbents to remove Cr(VI). It has been estimated that a kg of adsorbent is needed to remove a g of Cr(VI) from textile effluent (Sharma et al. 2021). The production of biosorbents is shown in a flowsheet in Fig. 8.

Table 6 outlines the cost of drying and grinding 1 kg of cocoa husk at a total of \$0.24.

The results show that employing agricultural waste as an adsorbent is less expensive than using commercial AC. AC for packed bed columns has been estimated to cost \$1,855/m^3 (Loh et al. 2002). The adsorptions placed in the lower section of the column are designed to remove specific pollutants, such as Cr(VI), from wastewater (Ren et al. 2011).

Estimated capital cost (CAPEX)

CAPEX is defined as one-time expenditures on the enhancement, construction and acquisition of assets such as land and equipment installation, that will benefit the project for a long time and is categorised into sections (Towler and Sinnott 2021). The equations used to find CAPEX are compiled in Table 7.

CAPEX is the sum of fixed capital investment (FCI) and working capital investment (WCI). The FCI represents the total cost a company spends on those elements associated with the construction, designing, commissioning and installation of a plant. These elements belong to the company and can be used for long to receive benefits beyond the current accounting period (Sloman et al. 2019). The FCI consists of four major categories: inside battery limit (ISBL), outside battery limits (OSBL), contingency cost and design and engineering (D&E) costs.

ISBL refers to the total cost that needs to be spent on purchasing and installing all process equipment such as land costs, piping, catalysts, shipping costs of equipment and any other material associated with the construction of the plant,

Fig. 9 Fixed bed column cost estimation curve plus installation costs (Loh et al. 2002)

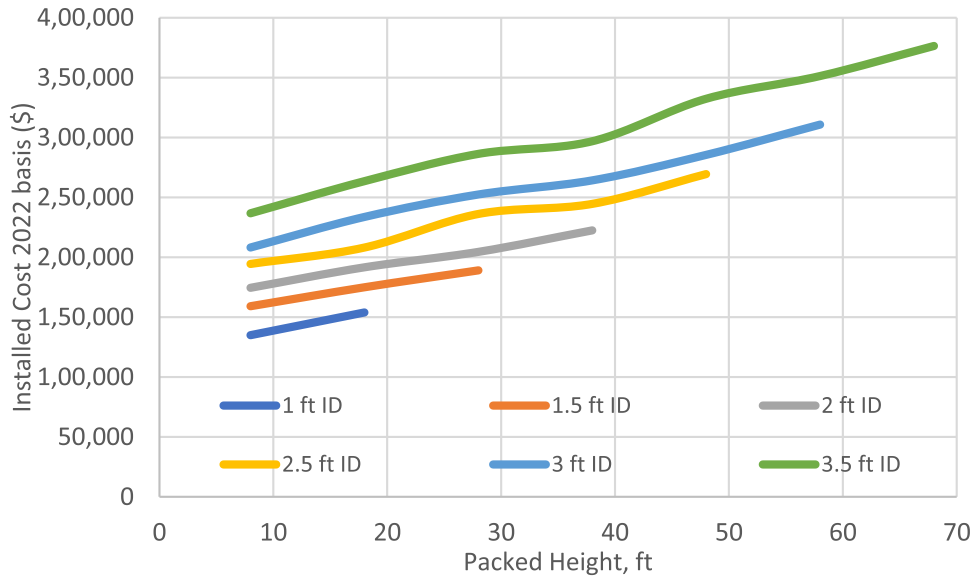

or final plant operation. Since the focus of the economic study is on the fixed bed column, the total ISBL is the cost of the column. Using a cost curve for a packed bed column with a design pressure of 15 psig (1.02 atm) and 1998 design basis, the installed cost of a packed bed column for scenarios 1 and 2 was \$73,000 and \$178,500, respectively (Loh et al. 2002). This cost will be updated to reflect inflation to a more modern value using temporal factors. The column in scenario 2 is \$105,500 more expensive due to the increased bed height and diameter. The cost curve can be seen in Fig. 9.

To convert the ISBL cost from the year 1998 into the year 2022, the chemical engineering plant cost index (CEPCI) for the relevant year is used. The CEPCI for 1998 is 389.5 (Loh et al. 2002). The CEPCI for September 2022 is 821.3 (Maxwell 2020). Equation 4 was used to reflect the ISBL cost in more modern times (Towler and Sinnott 2021; Sloman et al. 2019).

The OSBL is acquired as 40% of the ISBL value, shown in Eq. 5 (Towler and Sinnott 2021). The contingency cost is evaluated as 10% of ISBL + OSBL as displayed in Eq. 6 (Towler and Sinnott 2021). The D&E cost is the total cost of engineering, designing and any material related to the structuring of the project internally or externally (Towler and Sinnott 2021). It is calculated as 20% of the ISBL + OSBL value, shown in Eq. 7. Thus, to calculate FCI, Eq. 8 is used.

The value for WCI can be evaluated as 5% of the total ISBL + OSBL if the size of the plant is a relatively small and non-chemical project (Towler and Sinnott 2021). For this case, Eq. 9 is applied. Therefore, the total CAPEX can be found using Eq. 10. The total CAPEX was \$290,924 and \$711,368 for scenarios 1 and 2, respectively. Scenario 2 is nearly two and a half times more expensive than scenario 1 for a wider column with 50 additional feet.

Operation expenditure (OPEX)

Operation expenditure (also known as operating expense) consists of the total money a company needs to spend to run a business or system smoothly daily. Hence, the depreciation of fixed assets used in the production process is considered OPEX expenditure (Sloman et al. 2019). OPEX is the total of the fixed costs of production (FCOP) and the variable cost

Table 8 Fixed cost of production

Variable	Equation	Value	Eq. No.
Labour cost	Only handling charge	Scenario 1: \$0 (no labour required) Scenario 2: \$0 (no labour required)	
Maintenance cost	$Maintenance\ = ISBL \times\ 0.03$	Scenario 1: $153,928 \times\ 0.03 = \$4,618$ Scenario 2: $376,385 \times\ 0.03 = \$11,292$	11
FCOP	$FCOP\ = Labour + Maintenance$	Scenario 1: $\$4,618$ Scenario 2: $\$11,292$	12

Table 9 Variable cost of production

Variable	Equation	Value	Eq. No.
Mass of bed	$m = 1/4 \times \pi \times D^2 \times h \times \rho$	Scenario 1: $\frac{1}{4} \times \pi \times 0.3048^2 \times 5.4864 \times 518 = 207\ kg$ Scenario 2: $\frac{1}{4} \times \pi \times 1.0668^2 \times 20.7264 \times 518 = 9,596\ kg$	13
Cost per bed	$Price = Price\ per\ kg \times m$	Scenario 1: $0.24 \times 207 = \$50$ Scenario 2: $0.24 \times 9,596 = \$2,303$	14
Beds used in 20y	$Beds_{20y} = \frac{630,720,000}{Breakthrough\ time\ (seconds)}$	Scenario 1: $\frac{630,720,000}{86,400} = 7300\ beds$ Scenario 2: $\frac{630,720,000}{2,419,200} = 261\ beds$	15
Bed cost for 20y	$VCOP_{20_y} = Beds_{20_y} \times Cost\ per\ bed$	Scenario 1: $7300 \times 50 = \$365,000$ Scenario 2: $261 \times 2,303 = \$601,083$	16
20y OPEX	$OPEX_{20_y} = FCOP_{20y} + VCOP_{20_y}$	Scenario 1: $20 \times 4,618 + 365,000 = \$457,360$ Scenario 2: $20 \times 11,292 + 601,083 = \$826,923$	17
The volume of clean water per bed	$Volume\ of\ water = Flow\ rate \times Breakthrough\ time\ (s)$	Scenario 1: $0.04545293 \times 86,400 = 3,927\ L$ Scenario 2: $0.61429526 \times 2,419,200 = 1,486,103\ L$	18
The volume of clean water 20y	$Clean\ water\ volume_{20y} = Volume\ per\ bed \times Beds_{20y}$	Scenario 1: $3,927 \times 7,300 = 28,667,100\ L$ Scenario 2: $1,486,103 \times 261 = 387,872,883\ L$	19

Table 10 Total CAPEX, OPEX and throughput for scenarios 1 and 2

Cost	Scenario 1	Scenario 2
CAPEX ($)	290,924	711,368
OPEX (20y) ($)	455,662	826,951
Total 20y Cost ($)	746,585	1,538,319
The volume of water processed in 20y (m3)	28,667	387,873
Value of clean water ($)	79,984	1,082,165

of production (VCOP). The term FCOP refers to a business expense that stays the same month to month, no matter how the size of sales increases or decreases. The FCOP consists of operation labour and maintenance costs (Towler and Sinnott 2021). The equations used to find FCOP can be seen in Table 8.

The operating labour cost can be estimated at $60,000 per year (Towler and Sinnott 2021). The labour cost can be ignored since the fixed bed column would be a small addition to an existing process system. The labour cost for 20 years would also overshadow the focus of the economic study which is investigating two columns with different parameters and their processing costs. The maintenance cost could be calculated as 3% of ISBL by using Eq. 11 (Towler and Sinnott 2021). Thus, the total cost of FCOP can be found using Eq. 12. The FCOP was $4618 and $11,292 for scenarios 1 and 2, respectively. Since scenario 2 uses a bigger column, the FCOP is $6,674 more expensive.

In the VCOP section, the cost analysis for three columns with different breakthrough times will be compared. The VCOP is broken down in Table 9. The cost of the cocoa husk pod to fill the beds is required to find VCOP. Cocoa pod husk costs $0.24 per kg. The mass of the cocoa husk required to fill the fixed bed columns was found using Eq. 13 (Adornado et al. 2016). Where m is the mass of the adsorbent in the bed (kg); D is the internal diameter of the bed (m); h is the height of the bed (m) and ρ is the density of the adsorbent (kg/m^3). Bed 1 and 2 had a mass of 207 kg and 9,596 kg, respectively. The bed in scenario 2 is nearly 50 times heavier than in scenario (1) The mass of the bed and Eq. 14 is used to calculate the total cost for a full bed for scenario 1 and (2) This study uses a range of 20 years to evaluate the scenarios. The total number of beds used in the 20 years is calculated using Eq. 15. It is assumed once the breakthrough time is reached and the outlet concentration of chromium reaches 5%, the bed needs to be replaced. The bed in Scenario 1 lasts for 1 day before meeting its breakthrough time, this means

7300 beds are required over 20 years. The bed in Scenario 2 lasts for 4 weeks and requires 261 beds over 20 years. Therefore, the cost of the beds can be calculated using Eq. 16, with Scenario 1 costing 65% more than Scenario 2. The 20-year OPEX can be calculated using Eq. 17. The total OPEX for scenarios 1 and 2 was $455,662 and $826,951, respectively. The difference in OPEX is significant due to the number of beds used in Scenario 1 in comparison to Scenario 2.

Equations 18 and 19 can be used to find the volume of water processed by the column over 20 years. The price of water in the US is on average at $2.79/m^3$ (Salas 2023). The total cost of both scenarios and the throughput of water over 20 years is summarised in Table 10.

Scenario 1 costs $746,585 and scenario 2 costs $1,538,319 over the 20 years. Scenario 1 had a lower capital and operating expenditure because it used a smaller-sized column and a lower mass of adsorbent. Scenario 1 will likely have additional ancillary costs not considered in the analysis due to adsorbent storage, transport and the cost of having to physically change the bed daily. Scenario 1 processed 28,668 m^3 of water and Scenario 2 processed 387,873 m^3. The value of water processed in Scenario 2 was 13.5 times greater than in Scenario 1. Scenario 2 processed the most water over the 20 years, this is because it had a high flow rate and breakthrough time. Using scenario 2 and ignoring capital cost and labour, the cost per m^3 of water throughput is $2.13/$m^3$, compared with a similar process using photocatalyst which costs $3.86/$m^3$ (Baaloudj et al. 2022). Due to the low cost of the adsorbent, the process is slightly cheaper to run than a photocatalyst process.

This study shows how simulation and RSM can be used in tandem to forecast the effectiveness of adsorbents and assist in economic analysis. It is shown that adjustments to key factors can affect the capital and operating cost, breakthrough time and water throughput. A major contributor to this outcome is the cheapness of the adsorbent material. If the price of $1,855/$m^3$ (AC) was used, then scenario 1 would cost $743 per bed and OPEX would be $5,513,290 over 20 years. The bed in scenario 2 would cost $34,366 and the OPEX over the 20 years would cost $9,195,248. Ultimately, the cost and throughput of the column will depend on the requirements of the process.

Conclusion

The present study shows that the scaled-up wastewater treatment process using low-cost adsorbents can be successfully evaluated and designed using data from computational simulation and optimisation software. The removal of Cr(VI) using cocoa pod husk biosorbent was simulated using Aspen Plus and optimised using Design Expert. Biosorbents are a viable alternative to conventional adsorbents, as they are less expensive and can be made from waste materials. The results of the simulation showed that a taller bed height (2.0 m), wider diameter (2.0 m) and lower flow rate (0.010 L/s) improved adsorption. Initial concentration had no effect when a relatively high flow rate and initial concentration were used. The variables were optimised using RSM to give a predicted breakthrough and saturation time of 29,360 and 313,351 s, respectively. Using the simulation and optimisation data, an economic study was carried out. Two scenarios with different column parameters were compared over 20 years using economic analysis. Scenario 1 (1 day breakthrough time) and Scenario 2 (4 weeks breakthrough time) cost $1,538,319 and $746,585, respectively. They processed 28,668 m^3 and 387,873 m^3 of water, respectively. Simulation software offers faster and cheaper solutions than its real-world counterpart. It can be used to replicate scenarios that would otherwise be unsafe or expensive to carry out. The accuracy of this method is dependent on the input data and the proficiency of the user. However, the method is limited. Simulations assume ideal conditions and may not encompass all possible variables. Future work includes investigating the effects of temperature, mixed pollutants and adsorption columns in series.

Acknowledgements We extend our gratitude to everyone who contributed insights and support for this work. No external funding was received, but the dedication of all involved has been invaluable.

Author contributions Formal analysis and investigation: Mathew C. Holliday, Faranak Esmati; Writing—original draft preparation: Mathew C. Holliday, Faranak Esmati, Sharif H. Zein; Writing—review and editing: Khalaf J. Jabbar, Soon Huat Tan, Aditya Putranto; Conceptualization and Supervision: Sharif H. Zein.

Funding The authors did not receive support from any organisation for the submitted work. No funding was received to assist with the preparation of this manuscript.

Data availability Not applicable.

Declarations

Conflict of interest The authors have no competing interests to declare that are relevant to the content of this article.

References

Adornado AP, Soriano AN, Orfiana ON, Pangon MBJ, Nieva AD (2016) Simulated biosorption of cd(II) and Cu(II) in single and binary metal systems by water hyacinth (*Eichhornia crassipes*) using Aspen Adsorption. ASEAN J Chem Eng 16(2):21–43. https://doi.org/10.22146/ajche.49892

Agarwal A, Upadhyay U, Sreedhar I, Anitha KL (2022) Simulation studies of Cu(II) removal from aqueous solution using olive stone. Clean Mater 5:100128. https://doi.org/10.1016/j.clema.2022.100128

Amiri MJ, Bahrami M, Beigzadeh B, Gil A (2018) A response surface methodology for optimization of 2,4-dichlorophenoxyacetic acid removal from synthetic and drainage water: a comparative study. Environ Sci Pollut Res 25:34277–34293. https://doi.org/10.1007/s11356-018-3327-x

Anisuzzaman SM, Bono A, Krishnaiah D, Tan YZ (2016) A study on dynamic simulation of phenol adsorption in activated carbon packed bed column. J King Saud Univ – Eng Sci 28(1):47–55. https://doi.org/10.1016/j.jksues.2014.01.001

Baaloudj O, Badawi AK, Kenfoud H, Benrighi Y, Hassan R, Nasrallah N, Assadi AA (2022) Techno-economic studies for a pilot-scale Bi12TiO20 based photocatalytic system for pharmaceutical wastewater treatment: from laboratory studies to commercial-scale applications. J Water Process Eng 48:102847. https://doi.org/10.1016/j.jwpe.2022.102847

Baaloudj O, Nasrallah N, Kenfoud H, Bourkeb KW, Badawi AK (2023) Polyaniline/Bi12TiO20 hybrid system for Cefixime removal by combining adsorption and photocatalytic degradation. ChemEngineering 7(1):4. https://doi.org/10.3390/chemengineering7010004

Badawi AK, Elkodous MA, Ali GAM (2021) Recent advances in dye and metal ion removal using efficient adsorbents and novel nano-based materials: an overview. RSC Adv 58. https://doi.org/10.1039/D1RA06892J

Badawi AK, Ismail B, Baaloudj O, Abdalla KZ (2022) Advanced wastewater treatment process using algal photo-bioreactor associated with dissolved-air flotation system: a pilot-scale demonstration. J Water Process Eng. https://doi.org/10.1016/j.jwpe.2022.102565

Badawi AK, Salama RS, Mostafa MMM (2023) Natural-based coagulants/flocculants as sustainable market-valued products for industrial wastewater treatment: a review of recent developments. RSC Adv. https://doi.org/10.1039/D3RA01999C

Bank of England (2023) Daily spot exchange rates against US Dollars. https://www.bankofengland.co.uk/boeapps/database/Rates.asp?Travel=NIxAZx&into=EUR (accessed 24 May

Calero M, Hernáinz F, Blázquez G, Tenorio G, Martín-Lara MA (2009) Study of Cr (III) biosorption in a fixed-bed column. J Hazard Mater 171:886–893. https://doi.org/10.1016/j.jhazmat.2009.06.082

Carvalho J, Araujo J, Castro F (2011) Alternative low-cost adsorbent for water and wastewater decontamination derived from eggshell waste: an overview. Waste Biomass Valoriz 2(2):157–167. https://doi.org/10.1007/s12649-010-9058-y

Chen S, Yue Q, Gao B, Xu X (2010) Equilibrium and kinetic adsorption study of the adsorptive removal of Cr(VI) using modified wheat residue. J Colloid Interface Sci 349(1):256–264. https://doi.org/10.1016/j.jcis.2010.05.057

Crini G, Lichtfouse E (2018) Advantages and disadvantages of techniques used for wastewater treatment. Environ Chem Lett 17:145–155. https://doi.org/10.1007/s10311-018-0785-9

Dawodu FA, Akpan BM, Akpomie KG (2020) Sequestered capture and desorption of hexavalent chromium from solution and textile wastewater onto low cost *Heinsia crinita* seed coat biomass. Appl Water Sci. https://doi.org/10.1007/s13201-019-1114-6

Dichiara AB, Weinstein SJ, Rogers RE (2015) On the choice of batch or fixed bed adsorption processes for wastewater treatment. Ind Eng Chem Res 54(34):8579–8586. https://doi.org/10.1021/acs.iecr.5b02350

Ehsanpour S, Samani MR, Toghraie D (2023) Removal of chromium (VI) from aqueous solution using eggshell/ poly pyrrole composite. Alex Eng J 64:581–589. https://doi.org/10.1016/j.aej.2022.09.018

González-Delgadoa ÁD, Tejada-Tovarb C, Villabona-Ortízb A (2022) Computer-aided modeling and evaluation of a packed Bed for Chromium (Vi) removal using residual biomass of *Theobroma Cacao* L. Chem Eng Trans 92:517–522. https://doi.org/10.3303/CET2292087

Guesmi A, Cherif MM, Baaloudj O, Kenfoud H, Badawi AK, Elfalleh W, Hamadi NB, Khezami L, Assadi AA (2022) Disinfection of corona and myriad viruses in water by non-thermal plasma: a review. Environ Sci Pollut Res Int 29(37):55321–55335. https://doi.org/10.1007/s11356-022-21160-7

Guo X, Liu A, Lu J, Niu X, Jiang M, Ma Y, Liu X, Li M (2020) Adsorption mechanism of hexavalent chromium on biochar: kinetic, thermodynamic, and characterization studies. ACS Omega 5(42):27323–27331. https://doi.org/10.1021/acsomega.0c03652

Hameed A, Hameed BH, Almomani FA, Usman M, Ba-Abbad MM, Khraisheh M (2019) Dynamic simulation of lead(II) metal adsorption from water on activated carbons in a packed-bed column. Biomass Conv Bioref. https://doi.org/10.1007/s13399-022-03079-8

Holkar CR, Jadhav AJ, Pinjari DV, Mahamuni NM, Pandit AB (2016) A critical review on textile wastewater treatments: possible approaches. J Environ Manage 182:351–366. https://doi.org/10.1016/j.jenvman.2016.07.090

Holliday MC, Parsons DR, Zein SH (2022a) Agricultural pea waste as a low-cost pollutant biosorbent for methylene blue removal: adsorption kinetics, isotherm and thermodynamic studies. Biomass Convers Biorefin. https://doi.org/10.1007/s13399-022-02865-8

Holliday MC, Parsons DR, Zein SH (2022b) Microwave-assisted hydrothermal carbonisation of waste biomass: the effect of process conditions on hydrochar properties. Processes 10:1756. https://doi.org/10.3390/pr10091756

Hosseini SA, Samani MR, Toghraie D (2021) Removal of hexavalent chromium from aqueous solution using ostrich feathers amended by polyaniline. J Mater Res Technol 15:488–499. https://doi.org/10.1016/j.jmrt.2021.08.041

Hougni D-GJM, Schut AGT, Woittiez LS, Vanlauwe B, Giller KE (2021) How nutrient rich are decaying cocoa pod husks? The kinetics of nutrient leaching. Plant Soil 463(1–2):155–170. https://doi.org/10.1007/s11104-021-04885-1

Johanto A, Cahyani VR, Rosariastuti R (2014) Bioremediation of paddy field contaminated by liquid waste from textile industry in order to reduce chromium in soil and rice plant. AIP Conference Proceedings. https://doi.org/10.1063/1.5054429

Kane A, Assadi AA, Jery AE, Badawi AK, Kenfoud H, Baaloudj O, Assadi AA (2022) Advanced photocatalytic treatment of wastewater using immobilized titanium dioxide as a photocatalyst in a pilot-scale reactor. Process Intensif Mater 15(13):4547. https://doi.org/10.3390/ma15134547

Kenfoud H, Nasrallah N, Baaloudj O, Meziani D, Chaabane T, Trari M (2020) Photocatalytic reduction of cr(VI) onto the spinel CaFe2O4 nanoparticles. Optik 223:165610. https://doi.org/10.1016/j.ijleo.2020.165610

Lingamdinne, Karri RR, Khan MR, Chang Y-Y, Koduru JR (2021) Evaluation of surface phenomena of magnetic biomass for dye removal via surface modeling. J Environ Chem Eng 9(5):105953. https://doi.org/10.1016/j.jece.2021.105953

Loh HP, Lyons J, White CW III (2002) Process equipment cost Estimation Final Report. National Energy Technology Lab, Morgantown

Maiti S, Purakayastha S, Ghosh B (2007) Production of low-cost carbon adsorbents from agricultural wastes and their impact on dye adsorption. Chem Eng Commun 195(4):386–403. https://doi.org/10.1080/00986440701707917

Mater Y, Kamel M, Karam A, Bakhoum E (2023) ANN-Python prediction model for the compressive strength of green concrete. Constr Innov 23(2):340–359. https://doi.org/10.1108/CI-08-2021-0145

Maxwell C (2020) Cost Indices. Towering Skills. https://toweringskills.com/financial-analysis/cost-indices/ (accessed 24 May, 2023)

Nieva A, Garcia R, Ped R (2019) Simulated biosorption of Cr6 + using peels of Litchi chinensis Sonn by Aspen Adsorption® V8.4. Int J Environ Sci Dev 10:331–337. https://doi.org/10.18178/ijesd.2019.10.10.1195

Nwabanne J, Okoye AC, Lebele-Alawa T (2011) Packed Bed Column studies for the removal of lead (II) using oil palm empty fruit bunch. Eur J Sci Res 63(2):296–305

Priyadharshini MR, Soundhirajan K (2021) Removal of chromium (VI) from textile waste Water by using activated carbon prepared from neem leaves and garlic husk. Middle East J Appl Sci Technol 4(3):19–28

Rafiaee S, Samani MR, Toghraie D (2020) Removal of hexavalent chromium from aqueous media using pomegranate peels modified by polymeric coatings: effects of various composite synthesis parameters. Synth Met 265:116416. https://doi.org/10.1016/j.synthmet.2020.116416

Rahim I, Jumardin J, Suherman S, Nasruddin A (2019) Biodegradation of cocoa pod husk waste used rot fungi consortium at various storage times. 1st Int Conf Sci Technol. https://doi.org/10.4108/eai.2-5-2019.2284691

Ren L, Zhang J, Li Y, Zhang C (2011) Preparation and evaluation of cattail fiber-based activated carbon for 2,4-dichlorophenol and 2,4,6-trichlorophenol removal. Chem Eng J 168(2):553–561. https://doi.org/10.1016/j.cej.2011.01.021

Salas EB Tap water prices in, Statista (2023) https://www.statista.com/statistics/1232861/tap-water-prices-in-selected-us-cities/ (accessed 24 May, 2023)

Saleh TS, Badawi AK, Salama RS, Mostafa MMM (2023) Design and development of novel composites containing nickel ferrites supported on activated carbon derived from agricultural wastes and its application. Water Remediat Mater 16(6):2170. https://doi.org/10.3390/ma16062170

Samani MR, Toghraie D (2019) Removal of hexavalent chromium from water using polyaniline/ wood sawdust/ poly ethylene glycol composite: an experimental study. J Environ Health Sci Eng 17:53–62. https://doi.org/10.1007/s40201-018-00325-y

Sarkar S, Das SK (2016) Removal of hexavalent chromium from aqueous solution using natural adsorbents---column studies. Int J Eng Res Technol https://doi.org/10.17577/IJERTV5IS110270

Shahzad W, Badawi AK, Rehan ZA, Khan AM, Khan RA, Shah F, Ali S, Ismail B (2022) Enhanced visible light photocatalytic performance of Sr0.3(Ba,Mn)0.7ZrO3 perovskites anchored on graphene oxide. Ceram Int 48(17):24979–24988. https://doi.org/10.1016/j.ceramint.2022.05.151

Sharma PK Ayub S, Shukla BK (2021) Cost and feasibility analysis of chromium removal from water using agro and horticultural wastes as adsorbents. In: 3rd Int Conf Innov Technol Clean Sustain Dev 29:449–463. https://doi.org/10.1007/978-3-030-51485-3_30

Sloman J, Garratt D, Guest J, Jones E (2019) Economics for Business, 8th edition. Pearson, London

Stat-Ease (2021) Inc. Design Expert Help

Sutradhar P, Maity P, Kar S, Poddar S (2019) Modelling and optimization of PSA (pressure swing adsorption) unit by using aspen Plus® and design expert ®. Int J Innov Technol Explor Eng 8(4):64–69

Thoppil Y, Zein SH (2021) Techno-economic analysis and feasibility of industrial-scale biodiesel production from spent coffee grounds. J Clean Prod 307:127113. https://doi.org/10.1016/j.jclepro.2021.127113

Towler G, Sinnott R (2021) Chemical Engineering Design principles, practice and economics of plant and process design third editon. Butterworth-Heinemann, Oxford

Upadhyay U, Gupta S, Agarwal A, Sreedhar I, Anitha KL (2023) Adsorptive removal of Cd2 + ions using dolochar at an industrial-scale process optimization by response surface methodology. Environ Sci Pollut Res Int 30(4):8403–8415. https://doi.org/10.1007/s11356-021-17216-9

Waudby H, Zein SH (2021) A circular economy approach for industrial scale biodiesel production from palm oil mill effluent using microwave heating: design, simulation, techno-economic analysis and location comparison. Process Saf Environ Prot 148:1006–1018. https://doi.org/10.1016/j.psep.2021.02.011

Yaseen DA, Scholz M (2019) Textile dye wastewater characteristics and constituents of synthetic effluents: a critical review. Int J Environ Sci Technol 16:1193–1226. https://doi.org/10.1007/s13762-018-2130-z

Yasir HA, Zein SH, Holliday MC, Jabbar KJ, Ahmed U, Jalil AA (2023) Comparison of activated carbon and low-cost adsorbents for removal of 2,4-dichlorophenol from wastewater using Aspen Adsorption and response surface methodology. Environ Technol https://doi.org/10.1080/09593330.2023.2202829

Zhang YP, Adi VSK, Huang H-L, Lin H-P, Huang Z-H (2019) Adsorption of metal ions with biochars derived from biomass wastes in a fixed column: adsorption isotherm and process simulation. J Ind Eng Chem. https://doi.org/10.1016/j.jiec.2019.03.046

Authors and Affiliations

F. Esmati[1] · M. C. Holliday[1,2] · S. H. Zein[1] · K. J. Jabbar[1] · S. H. Tan[3] · A. Putranto[4]

✉ S. H. Zein
s.h.zein@hull.ac.uk

1 School of Engineering, Faculty of Science and Engineering, University of Hull, Kingston Upon Hull HU6 7RX, UK

2 Energy and Environment Institute, University of Hull, Kingston Upon Hull HU6 7RX, UK

3 School of Chemical Engineering, Universiti Sains Malaysia, Engineering Campus, Seri Ampangan, Nibong Tebal, 14300 Seberang Perai Selatan, Pulau Pinang, Malaysia

4 School of Chemistry and Chemical Engineering, Faculty of Engineering and Physical Sciences, University of Surrey, Guildford GU2 7XH, UK